Heat capacity of ZnO: Isotope effects

J. Serrano,[1,*] R. K. Kremer,[2] M. Cardona,[2] G. Siegle,[2] A. H. Romero,[3] and R. Lauck[2]
[1]*European Synchrotron Radiation Facility, Boîte Postale 220, 38043 Grenoble, France*
[2]*Max Planck Institut für Festkörperforschung, Heisenbergstrasse 1, D-70569 Stuttgart, Germany*
[3]*CINVESTAV, Departamento de Materiales, Unidad Querétaro, Querétaro, 76230 Mexico*
(Received 18 November 2005; revised manuscript received 23 January 2006; published 9 March 2006)

We have measured the heat capacity of zinc oxide for several single crystals with different isotopic compositions in the 5–350 K temperature range. We have performed first-principles calculations in order to analyze the dependence of the heat capacity on the isotope mass of the oxygen and zinc atoms. This dependence provides us relevant information to understand thermodynamic properties from a microscopic point of view, and to validate theoretical models of phonon dispersion relations and atomic displacements. The Zn mass affects mainly the acoustic phonons, thus leading to isotopic effects on the heat capacity mostly at low temperatures, whereas the O mass affects mainly the optic phonons, which become thermally active at higher temperatures. This behavior is reproduced quantitatively by the calculations, and is also in agreement with theoretical predictions reported for wurtzite GaN, an isostructural semiconductor.

DOI: 10.1103/PhysRevB.73.094303 PACS number(s): 63.20.Dj, 65.40.Ba

I. INTRODUCTION

The availability of semiconductor crystals with different isotopic abundances has triggered profuse investigations[1] of the effect of isotopic composition on thermodynamic,[2,3] vibrational,[4] and electronic[5] properties. Most of this work, in particular the investigations of thermodynamic properties, is concerned with monatomic semiconductors, i.e., diamond, Si, Ge, and α-Sn. However, the effect of the isotopic masses in multinary compounds on the thermodynamic properties, such as the heat capacity at constant pressure, C_p, should depend on which mass is being considered. This has been recently pointed out in an article on the heat capacity of GaN (Ref. 3), though unfortunately no appropriate isotopic crystals of GaN were available. The isotopic mass dependence of the heat capacity in binary compounds provides a way to unveil the microscopic mechanisms involved in thermodynamic properties, and to validate theoretical models of the lattice dynamics beyond the simple description of phonon dispersion relations, since the atomic displacements contribute in a different way depending on which isotopic mass is varied.

Zinc oxide, similarly to GaN, is a wurtzitelike semiconductor. With applications in everyday life as sun blocker lotions, cosmetics, adhesive tapes, ceramics, and varistors,[6] it has an electronic band gap of 3.4 eV that makes it suitable for fabrication of optoelectronic devices in the ultraviolet range.[7] Therefore an appropriate characterization of the thermodynamic properties, such as the thermal conductivity and the heat capacity, is essential for the development of high-quality devices. Besides this, the relatively large mass difference between zinc and oxygen atoms, 4 to 1, provides an excellent scenario for testing isotopic effects and elucidating the contributions of oxygen and zinc displacements to the heat capacity. The similarities between ZnO and GaN, for which theoretical predictions were reported,[3] together with the availability of a sizable number of single crystals with different isotopic compositions, motivated further the choice of this material for the investigation of the isotopic effects on the heat capacity in binary compounds.

In this paper we report measurements of the heat capacity for ZnO, for which small single crystals with a wide range of isotopic abundances are available.[1] These crystals were reliably characterized by Raman[8] and luminescence[9] spectroscopy. We have performed extensive measurements of the heat capacity as a function of temperature for a number of these crystals, as well as *ab initio* calculations within the harmonic approximation based on their electronic structure and a local density approximation using density functional theory. We present measured curves of C_p vs T for several isotopic compositions and compare them with theoretical predictions. In earlier work on diamond,[10] silicon,[2] and germanium[11] the isotopic effects on the heat capacity C_p were illustrated by plotting the logarithmic derivative of C_p/T^3 with respect to average isotopic mass. Such plots exhibit a peak at a temperature of the order of 6% of the Debye temperature. As demonstrated theoretically in Ref. 3, this peak splits into two for binary crystals with different cationic and anionic masses, e.g., GaN. Here we present similar calculations for ZnO and compare them with experimental results. It is shown that the logarithmic derivative of C_p/T^3 with respect to the zinc mass peaks at $\approx$20 K whereas such a derivative with respect to the much lighter oxygen mass peaks at $\approx$160 K. These peaks are related to the mass dependence of acoustic and optic phonons, respectively.

II. THEORETICAL DETAILS

Ab initio calculations of the heat capacity at constant volume, C_V, were carried out for several isotopic compositions. With this aim we used 14 dynamical matrices corresponding to a grid of $6\times6\times3$ grid of $\mathbf{q}$ points in the irreducible Brillouin zone (BZ), obtained by linear response calculations based on density functional perturbation theory and a pseudopotential approximation using the code ABINIT.[12,13] These dynamical matrices allowed us to interpolate the force constants and obtain reasonably accurate data for the phonon dispersion relations and densities of states (DOS) as reported

in Ref. 8, where all the technical details are available. From these dynamical matrices we calculated the temperature dependence of the free energy, $F(T)$, and the heat capacity, C_V.[14] The evaluation of these thermodynamic properties requires one to know the full phonon dispersion relations and DOS, as shown in Eqs. (1) and (2):

$$F(T) = -\int_0^\infty \left(\frac{\hbar\omega}{2} + k_B T \ln[2n_B(\omega)]\right)\rho(\omega)d\omega, \quad (1)$$

$$C_V(T) = -T\left(\frac{\partial^2 F}{\partial T^2}\right)_V, \quad (2)$$

where k_B is the Boltzmann constant, n_B the Bose-Einstein factor, and $\rho(\omega)$ the phonon DOS, which actually defines the upper limit of the integral. As discussed in Ref. 3, the difference between C_p and C_V is significant only at high temperatures, and thus negligible in our temperature range.

The dependence on isotope mass was introduced at the level of the dynamical matrices, therefore assuming a negligible contribution of the change of the electronic structure, i.e., bonding, with isotopic composition. This ansatz is reasonable given the small effect of the thermal expansion on the average electronic band structure. It is also proven right *a posteriori* in view of the quantitative agreement between calculated and experimental data.[8,15]

For binary compounds, one can prove within the Debye model and the harmonic approximation that the logarithmic derivatives with respect to the isotopic mass at $T=0$ K should behave like

$$\frac{d\ln(C_V/T^3)}{d\ln M_{Zn}} = \frac{3}{2}\frac{M_{Zn}}{M_{Zn}+M_O} \approx 1.3, \quad (3)$$

$$\frac{d\ln(C_V/T^3)}{d\ln M_O} = \frac{3}{2}\frac{M_O}{M_{Zn}+M_O} \approx 0.2, \quad (4)$$

where we used as average masses ^{66}Zn and ^{17}O isotopic compositions.

In order to achieve convergence in the heat capacity and the logarithmic derivative with respect to the isotopic mass, a grid of $80\times80\times40$ **q** points in the irreducible BZ was employed for the evaluation of the integrals corresponding to the phonon DOS and the thermodynamic properties. This grid corresponds to a tolerance in the relative change of the DOS and C_V of 10% and 6%, respectively.[16] The number of points used in the integration is especially relevant for the convergence of the calculations of the logarithmic derivatives at low temperature. These calculations were performed by taking the finite differences of the calculated C_V for two different zinc and oxygen isotopic compositions. The dependence of the calculations on the chosen values for the zinc and oxygen masses was proven to be negligible and the low-temperature limits shown by Eqs. (3) and (4) were reproduced.

TABLE I. Compilation of the relevant data of all investigated ^{p}Zn^{q}O crystals.

Sample no.	mass (mg)	p (amu)	q (amu)
1	13.06	65.4	16
2	15.33	68	18
3	12.03	68	16
4	7.50	64	16
5	13.22	65.4	16/18 (1:1)
6	21.98	64/68 (1:1)	18
7	16.21	68	16/18 (1:1)
8	14.99	64	18
9	20.96	64/68 (1:1)	18
10	22.45	64	16/18 (1:1)

III. EXPERIMENTAL METHOD AND DATA TREATMENT

ZnO single crystals were grown by chemical vapor transport, using ammonium chloride as transport agent.[15,17,18] We have combined the highly enriched zinc isotopes ^{64}Zn (99.4%) and ^{68}Zn (97.9%), and natural zinc, with the isotope ^{18}O (99%) and natural oxygen ^{16}O (99.76%). Also compounds of 1:1 isotope mixtures were prepared, with a concentration of 50 ± 2 % for each isotope. In each case, purification, synthesis, and crystal growth were performed in the same ampoule from small quantities of materials. The purification of Zn was achieved by sublimation of the metal at temperatures of 350–500 °C. This procedure led to a thin solid zinc layer which favored the synthesis of ZnO in an O_2 atmosphere at temperatures above 500 °C. At a source temperature of 900–1000 °C and in an argon environment, we have obtained a limited number of pyramidlike and prismlike crystals with lengths up to 6 mm in the temperature range between 550 and 950 °C. The transparent crystals, grown at rates of 1–6 mg h^{-1} cm^{-2}, are colorless, yellowish, amber, or brownish, the color being attributed to defects such as oxygen vacancies.

The heat capacities in the temperature range $5<T<350$ K were measured using a Physical Property Measurements System calorimeter (Quantum Design, 6325 Lusk Boulevard, San Diego, CA.) employing the relaxation method. To thermally anchor the crystals to the sample platform, a minute amount ($\approx$0.3 mg) of Apiezon N vacuum grease was used. The heat capacity of the platform and grease was individually determined in a separate run and subtracted from the measured total heat capacities.

Table I summarizes the isotopic abundances corresponding to the ZnO crystals employed for heat capacity measurements. Typically a well-shaped crystal with a mass varying between $\approx$7 and $\approx$20 mg was selected. The size of the crystal was chosen such that at 5 K the heat capacity of the sample was about the same as that of the addenda, i.e., the

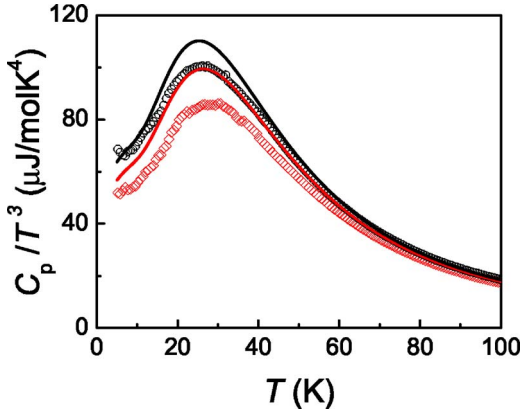

FIG. 1. (Color online) Experimental (○, ◇) and calculated (solid lines) heat capacities of $^{68}Zn^{18}O$ and of $^{64}Zn^{16}O$. Upper (black) solid line (○, sample no. 4), $^{68}Zn^{18}O$; lower (red) solid line (◇, sample no. 2), $^{64}Zn^{16}O$.

total heat capacity of the system formed by the sample platform plus the Apiezon vacuum grease.

In order to obtain the logarithmic derivative $d\ln(C_p/T^3)/d\ln M$ for a specified temperature T_0 the quantity $\ln[C_p(T_i)/T_i^3]$ (see, e.g., Fig. 1) was calculated from the experimental data of each sample listed in Table I, i.e., $\ln[C_p(T_0)/T_0^3]$ was calculated by using a polynomial of second order in T the coefficients of which had been fitted to all data points in the interval $T_0-5<T<T_0+5$ K. The derivative $d\ln(C_p/T^3)/d\ln M$ with respect the mass of either the Zn or the O isotope was then obtained as the slope of a straight line fitted to the plotted values of $\ln(C_p/T^3)$ versus $\ln M_{Zn,O}$ (cf., e.g., Refs. 1 and 2).

IV. DISCUSSION

Figure 1 shows the heat capacity obtained for two single crystals with $^{64}Zn^{16}O$ and $^{68}Zn^{18}O$ isotopic compositions. This figure illustrates the measurements performed on the samples described in Table I, which have values of C_V/T^3 lying between the two curves on Fig. 1. Generally, the larger the isotopic masses are, the smaller the phonon frequencies. Hence, a red shift of ≈2 K of the peak of C_V/T^3 is observed from $^{64}Zn^{16}O$ to $^{68}Zn^{18}O$. The calculated shift is ≈1.1 K, however the peak positions agree within 2 K with respect to the experimental values, $T\approx 26.5$ and 28.5 K, respectively. The increase of peak strength in C_V/T^3 with increasing isotopic mass occurs due to a decrease in the minimum of the Debye temperature $\theta_D(T)$ as observed in monatomic crystals such as silicon.[2] The maximum change of C_V/T^3 amounts to $15(1)\mu J/\text{mol K}^4$, corresponding to samples no. 2 and no. 4 (shown in Fig. 1), whereas the calculations show a change of $\approx 11\ \mu J/\text{mol K}^4$.

Figure 2 displays the logarithmic derivative of C_p/T^3 with respect to the mass of zinc isotope for all measured samples (see Table I) grouped into blocks with different oxygen mass. A sharp peak is observed at ≈22 K that corresponds to acoustic vibrations, associated mainly with displacements of zinc atoms. The larger mass of zinc with respect to that of

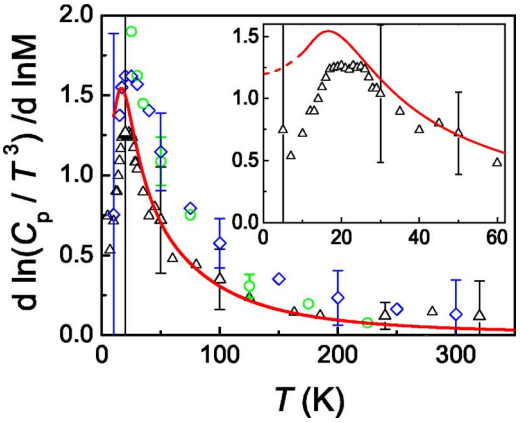

FIG. 2. (Color online) Logarithmic derivatives $d\ln(C_p/T^3)/d\ln M$ with respect to the mass of the Zn isotope. Solid (red) line, result of the theoretical calculation. Experimental data (black △) $^{p}Zn^{16}O$ ($p=64$, 65.4, 68; samples no. 4, no. 1, and no. 3, respectively); (green ○) $^{p}Zn^{16/18}O$ ($p=64$, 65.4, 68; samples no. 10, no. 5, and no. 7, respectively); (blue ◇) $^{p}Zn^{18}O$ ($p=64$, 66, 66, 68; samples no. 8, no. 6, no. 9, and no. 2, respectively). The inset shows the data for $^{p}Zn^{16/18}O$ in an enlarged scale, together with the calculation, and the dashed line corresponds to the extrapolation to the low-temperature limit [see Eq. (3)].

oxygen explains the presence of this peak at low temperatures. The inset shows a blowup of the maximum region, where the increasing difficulty to extract the sample heat capacity at low temperatures from that of the system formed by sample and platform is reflected in the larger error bars with decreasing temperature. The *ab initio* calculations agree well with the experimental data at temperatures larger than 100 K. At low temperatures the peak position is described in a qualitative way by the calculations, although the latter yield the maximum at 4 K lower temperature than the experimental data. The dashed line in the inset of Fig. 2 displays the extrapolation to $T=0$ K of the theoretical curve, in agreement with Eq. (3). At high temperature, the contribution

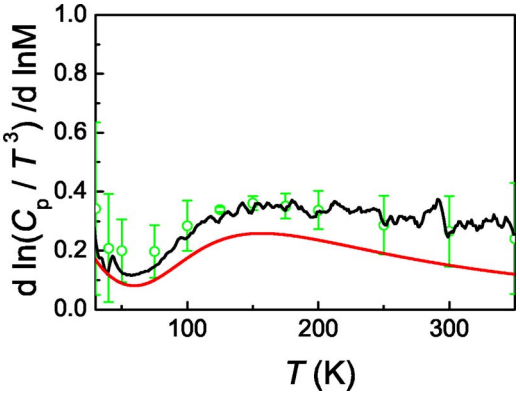

FIG. 3. (Color online) Logarithmic derivatives with respect to the mass of the oxygen isotope, $d\ln(C_p/T^3)/d\ln M_O$. Lower solid (red) line, result of the theoretical calculation. Upper solid (black) line, average of four derivatives with respect to the mass of the oxygen isotope. Open circles (green ○), derivative with respect to the mass of the oxygen isotope for the set $^{64}Zn^{q}O$ ($q=16,16/18,18$, samples no. 4, no. 10, and no. 8, respectively).

due to the displacements of zinc atoms becomes negligible and the logarithmic derivative decays exponentially.

The temperature dependence of the logarithmic derivative of C_p/T^3 with respect to the oxygen mass is displayed in Fig. 3, where two distinct maxima are observed at ≈20 and 160 K. The first maximum corresponds to transverse acoustic vibrations of ω close to zero, which behave as sound waves and the atomic displacements depend on the total mass. Therefore they are also slightly affected by the oxygen mass. This maximum depends on the possible inhomogeneity of the isotopic distribution of Zn atoms and overlaps with the maximum observed in Fig. 2. This is shown in Fig. 3 by the difference between the upper solid line, corresponding to an average between four derivatives with respect to the oxygen isotope, and the open circles, corresponding to the set $^{64}Zn^qO$, obtained from samples no. 4, no. 8, and no. 10. Besides this low-temperature peak, there is a broad asymmetric band with a maximum at 160 K. This band is related to the activation of lattice vibrations that predominantly involve displacements of oxygen atoms. The much smaller mass of oxygen as compared to that of zinc is responsible for the higher frequency of these modes, which in turn require a higher activation temperature. The calculations, displayed by the lower solid curve on Fig. 3, describe remarkably well the behavior of $d\ln(C_p/T^3)/d\ln M$ as a function of temperature, taking into account the strength of $d\ln(C_p/T^3)/d\ln M$, the limited accuracy of the calculation of the logarithmic derivatives, and the error bars present at low and high temperatures. A similar two-maxima behavior was predicted for GaN for the temperature dependence of the logarithmic derivative of C_p/T^3 with respect to the nitrogen mass in Ref. 3.

The purpose of this work was, in part, to corroborate similarities and differences between the dependence of heat capacities on isotope masses between monatomic crystals and similar materials with more than one chemically different atom. Such similarities and differences were discussed in Ref. 3 for α-GaN, for which isotopically modified crystals of sufficient size for heat capacity measurements were not available. In the present work we have investigated a considerable number of isotopically modified crystals of wurtzite ZnO, a material whose lattice dynamics and electronic structure is rather similar to that of α-GaN. Concerning the problem at hand, the basic difference between a monatomic and a diatomic crystal is that in the former the derivative of the heat capacity C_V with respect to isotopic mass can be obtained through simple differentiation of $C_V(T)$ vs T:

$$\frac{d\ln(C_V/T^3)}{d\ln M} = \frac{1}{2}\left(\frac{d\ln(C_V/T^3)}{d\ln T} + 3\right). \tag{5}$$

Equation (5) can be evaluated for monatomic crystals from the phonon DOS [see Eq. (1)] without any additional details about the lattice dynamics (e.g., the phonon eigenvectors).

As illustrated in Fig. 4, this is not possible for binary or multinary materials (see also Fig. 3 of Ref. 3). Figure 4 displays the calculated logarithmic derivatives $d\ln(C_V/T^3)/d\ln M_{Zn,O}$ (dashed lines) together with the result obtained by differentiating $\ln(C_V/T^3)$ with respect to temperature for the average of the two curves shown in Fig. 1, thus following the right-hand side (RHS) of Eq. (5). It also displays the corresponding theoretical temperature derivative. As already mentioned in Ref. 3, the sum of the calculated M_{Zn} and M_O derivatives coincides with the calculated temperature derivative, thus reproducing the behavior found for monatomic crystals. The shape of each of the mass derivative curves, however, is rather different. That calculated with Eq. (5) displays only one sharp peak at $T \approx 18$ K. In the actual partial derivatives this peak splits into two, one for the M_{Zn} derivative, at ≈20 K, and a broader one for the M_O derivative at ≈160 K. In order to obtain these partial derivatives with an expression similar to Eq. (5), some knowledge about the corresponding phonon eigenvectors would be needed. A general argument to explain these differences between both partial derivatives is that the zinc components of the eigenvectors are larger for the phonons with lower frequencies, and vice versa, whereas the opposite situation happens for the oxygen components. The agreement found between measured and calculated curves of $d\ln(C_{p,V}/T^3)/d\ln M_{Zn,O}$ shown in Figs. 2 and 3 also reflects the quality of the *ab initio* calculations.

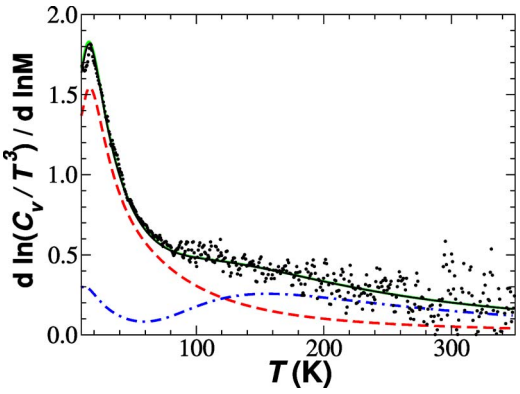

FIG. 4. (Color online) Calculated logarithmic derivatives $d\ln(C_p/T^3)/d\ln M$ with respect to M_{Zn} (red, dashed) and M_O (blue, dot-dashed), sum of both curves (green, solid), and RHS of Eq. (5) (black, solid), the latter obtained from an average of C_V on the 68/18 and 64/16 isotopic compositions. The filled circles (●) correspond to the application of the RHS of Eq. (5) on the same average of experimental data shown in Fig. 1. Note that the sum of the values plotted by the two dashed curves amounts to those shown by the solid black curve.

In summary, we have measured the heat capacity of ZnO in the 5–350 K temperature range on single crystals with a wide spread of isotopic compositions. The peak of C_p/T^3 shifts to lower temperature and increases in strength with increasing isotopic mass, in agreement with previous observations on monatomic semiconductors. There is a distinct behavior of the temperature dependence of the logarithmic derivatives of C_p/T^3 with respect to Zn and O masses, which stems from the contribution of Zn and O atomic displacements to the lattice vibrations and the activation of the latter at different temperatures. This behavior, as well as the heat capacity, are reasonably well reproduced by *ab initio* calculations that we have performed within the harmonic approxi-

mation. With increased accuracy, which would require larger isotopic samples, it should be possible to extract from the measured mass derivatives the spectral dependence of the density of phonon states projected on the constituent atoms, i.e., multiplied by the corresponding average eigenvector components.

ACKNOWLEDGMENTS

Thanks are due to H. Mattausch for a critical reading of the manuscript and to K. Graf for help with the data processing. A.H.R. acknowledges support by Conacyt Mexico under Grant No. J-42647-F.

*Electronic address: jserrano@esrf.fr

[1] M. Cardona and M. Thewalt, Rev. Mod. Phys. (to be published).
[2] A. Gibin, G. G. Devyatykh, A. V. Gusev, R. K. Kremer, M. Cardona, and H.-J. Pohl, Solid State Commun. **133**, 569 (2005).
[3] R. K. Kremer, M. Cardona, E. Schmitt, J. Blumm, S. K. Estreicher, M. Sanati, M. Bockowski, I. Grzegory, T. Suski, and A. Jezowski, Phys. Rev. B **72**, 075209 (2005).
[4] M. Cardona and T. Ruf, Solid State Commun. **117**, 201 (2001).
[5] C. Parks, A. K. Ramdas, S. Rodriguez, K. M. Itoh, and E. E. Haller, Phys. Rev. B **49**, 14244 (1994).
[6] H. E. Brown, *Zinc Oxide: Properties and Applications* (Pergamon Press, New York, 1976).
[7] X. L. Guo, J. H. Choi, H. Tabata, and T. Kawai, Jpn. J. Appl. Phys., Part 2 **40**, L177 (2001).
[8] J. Serrano, A. H. Romero, F. J. Manjón, R. Lauck, M. Cardona, and A. Rubio, Phys. Rev. B **69**, 094306 (2004).
[9] F. J. Manjón, M. Mollar, M. A. Hernandez-Fenollosa, B. Mari, R. Lauck, and M. Cardona, Solid State Commun. **128**, 35 (2003).
[10] M. Cardona, R. K. Kremer, M. Sanati, S. K. Estreicher, and T. R. Anthony, Solid State Commun. **133**, 465 (2005).
[11] W. Schnelle and E. Gmelin, J. Phys.: Condens. Matter **13**, 6087 (2001).
[12] X. Gonze *et al.*, Comput. Mater. Sci. **25**, 478 (2002).
[13] X. Gonze *et al.*, Z. Kristallogr. **220**, 558 (2005).
[14] X. Gonze, G.-M. Rignanese, and R. Caracas, Z. Kristallogr. **220**, 458 (2005).
[15] J. Serrano, F. J. Manjón, A. H. Romero, F. Widulle, R. Lauck, and M. Cardona, Phys. Rev. Lett. **90**, 055510 (2003).
[16] This corresponds to dostol=0.12 and thmtol=0.06 within the program anaddb of ABINIT. The ABINIT code is a common project of the Université Catholique de Louvain, Corning Incorporated, and other contributors (URL: http://www.abinit.org).
[17] M. Shiloh and J. Gutman, J. Cryst. Growth **11**, 105 (1971).
[18] K. Matsumoto and G. Shimaoka, J. Cryst. Growth **86**, 410 (1988).